

Leveraging User-Diversity in Energy Efficient Edge-Facilitated Wireless Collaborative Computing

Antoine Paris, Hamed Mirghasemi, Ivan Stupia and Luc Vandendorpe
ICTEAM/ELEN/CoSy, UCLouvain, Louvain-la-Neuve, Belgium

Abstract

In this work, a heterogeneous set of wireless devices sharing a common access point (AP) or base station (BS) collaborates to complete a set of computing tasks within a given deadline in the most energy-efficient way. This pool of devices somehow acts like a distributed mobile edge computing (MEC) server to augment the computing capabilities of individual devices while reducing their total energy consumption. Using the Map-Reduce distributed computing framework – which involves both local computing at devices and communications between them – the tasks are optimally distributed amongst the nodes, taking into account their diversity in term of computing and communications capabilities. In addition to optimizing the computing load distribution, local parameters of the nodes such as CPU frequency and RF transmit power are also optimized for energy-efficiency. The corresponding optimization problem can be shown to be convex and optimality conditions offering insights into the structure of the solutions can be obtained through Lagrange duality theory. A waterfilling-like interpretation for the size of the computing task assigned to each node is given. Numerical experiments demonstrate the benefits of the proposed optimal collaborative-computing scheme over various other schemes in several respects. Most notably, the proposed scheme exhibits increased probability of successfully dealing with larger computing loads and/or smaller latency and energy-efficiency gains of up to two orders of magnitude. Both improvements come from the scheme ability to optimally leverage devices diversity.

Index Terms

wireless collaborative computing, distributed computing, Map-Reduce, energy-efficiency, mobile edge computing, joint computation and communications optimization.

Corresponding author: antoine.paris@uclouvain.be.

I. INTRODUCTION

The current trends in communications and networking suggest that the future wireless ecosystem will be populated by a massive number of heterogeneous (in term of computing and communication capabilities) devices; from relatively powerful smartphones and laptops to ultra-low-power sensors, actuators and other connected “things” [1]. At the same time, emerging applications like virtual and augmented reality, machine learning and artificial intelligence, context-aware computing, autonomous driving, Internet of things (IoT) and so forth, require more and more computing capabilities while aiming for smaller and smaller latency. All in all, recent years have seen the focus moving from communications as an objective in itself to communications as a way to enhance computing capabilities of resources and energy limited devices [2], [3].

This paradigm shift first started with mobile cloud computing (MCC), that is, computation offloading to remote, centralized and immensely powerful cloud servers [4]. MCC proved itself to be effective to enable ubiquitous computing on limited devices while prolonging their battery life by moving the energy burden associated with the computing tasks to the cloud. However, with the ever growing number of connected devices and their ever growing computing demand, this solution is expected to suffer from long backhaul latency, rendering it unsuitable for ultra-low-latency applications emerging from the recent 5G developments.

More recently, mobile edge computing (MEC) has been introduced to avoid this unacceptable backhaul latency [5]–[7]. MEC relies on the deployment of small cloud-like computing servers at the edge of the network, i.e., at access points (AP), base stations (BS) or gateway in the context of low-power wide-area networks (LPWAN). These MEC servers are then exploited in the same way the cloud is in the context of MCC to augment the computing capabilities of limited devices while prolonging their battery life. At the opposite of MCC however, MEC has the advantage of offering smaller computing latency thanks to the proximity of MEC servers. Compared to MCC, MEC also has the advantage of offering some level of decentralization.

In this work, we further decentralize the computing resources by replacing the traditional MEC server located at the AP/BS by a pool of heterogeneous devices wirelessly connected to the AP/BS. Through collaborative computing and with the help of the AP/BS to facilitate communications between devices, coordinate the collaboration, and store data shared among the nodes, those distributed computing resources can also be exploited to enhance the computing capabilities of individual devices. In this scenario, computations are still performed on devices

rather than offloaded to powerful MEC or cloud servers, whose energy consumption are mostly ignored in existing works. As such, one cannot expect this solution to compete with MEC or MCC in term of devices energy savings. Nevertheless, in contexts where MCC latency is unacceptable and in the absence of MEC servers nearby or when the use of third-party owned MCC or MEC server is deliberately ruled-out for privacy reasons, investigating the potential benefits of pooling devices to augment their individual computing capabilities through collaborative computing still makes sense. This solution could also be integrated in a multi-tier architecture comprising devices collaborative-computing (which could be seen as a distributed MEC server architecture), MEC and MCC [8].

To model this collaborative computing scenario, we consider a set of N devices (also called nodes in the remaining of this paper), indexed by the letter $n \in [N]$ sharing a common access AP or BS. Under a given latency constraint τ , each node n wants to compute a certain function $\phi(d_n, w)$ where $d_n \in [0, 1]^D$ is some D -bit local information available to node n (e.g., sensed information, local state or context) and $w \in [0, 1]^L$ is a L -bit file with $L \gg D$ bits (e.g., a dataset) that might, for instance, be cached at the AP [9]. In the context of smart cities or smart buildings, w could be the result of the aggregation over space and time of information sensed from the environment through a network of sensors (e.g., traffic density or temperature) whereas the nodes could be actuators having some local state d_n that periodically need to perform some latency-sensitive computations to decide whether to take some actions (e.g., smart traffic lights or smart thermostats). Instead of each node n individually computing $\phi(d_n, w)$ – which might be prohibitive both in term of time and energy – nodes can work together to achieve their common objective. To this effect, a distributed computing framework such as Map-Reduce [10] can be used. In a nutshell, this framework divides the large file w (or equivalently, the computing load) among the nodes that then locally compute and subsequently exchange intermediate values that are finally locally combined inside each node to get the final output. This collaborative computing model thus involves local computations at the nodes and communication between the nodes via the AP/BS (i.e., the edge of the network is *facilitating* the communication between the nodes).

A. Contributions

The main contributions of this paper can be summarized as follows:

- we propose an N -node edge-facilitated collaborative-computing scheme based on the Map-Reduce distributed computing framework [10] and formulate an optimization problem to

make the whole N -node system as energy-efficient as possible ;

- we derive the feasibility condition of this problem, recast it to make it convex, gain engineering insights into the structure of the optimal solution by leveraging Lagrange duality theory and offer a waterfilling-like interpretation for the size of the computing task assigned to each node ;
- through numerical experiments, we compare the performance of the proposed scheme with various other schemes using less degrees-of-freedom in the optimization (such as the one proposed in [11]) and show that the proposed scheme optimally exploits nodes diversity.

B. Previous works

This paper extends our previous work [11] with a more realistic energy consumption model and more degrees of freedom in the optimization of the collaborative-computing scheme. This new work can actually be particularized to our previous one (see Sec. V for comparison of both works).

Wireless distributed-computing (WDC) was already vastly studied in the literature, mostly from an information theoretic point of view [12]–[15]. These works mainly focus on *coded distributed computing* (CDC) and study the trade-off between the computation and communication loads incurred by the collaboration. In short, increasing the computing load on the nodes makes it possible to leverage network coding opportunities during the exchange of intermediate values, hence reducing the communication load. In this work, we shift focus towards optimizing the collaborative-computing scheme to minimize the total energy consumption of the nodes.

The problem setup and collaborative computing model used in this work essentially follows [12]–[15], with the exception that we consider the set of nodes to be *heterogeneous* in term of computing and communications capabilities. As a consequence of this heterogeneity, it might no longer be optimal to uniformly distribute the computing load w across the nodes as is done in most previous works. To allow our collaborative-computing scheme to take into account – and leverage – the diversity of the nodes, our model thus allows arbitrary partition of the computing load w across the nodes. Compared to previous works on CDC, we also make the latency constraint accompanying the computing task explicit.

Various cooperative-computing schemes were already studied in the literature, see e.g., [16]–[21] discusses cooperative-computing and cooperative communications in the context of MEC systems wherein a user can partially (or totally) offload a computing task to both a MEC server

and a so-called helper node that can then (i) perform some local computations for the user node (i.e., cooperative computing), (ii) further offload part or all the task to the MEC server (i.e., cooperative communication), or (iii) both. The system model and problem formulation used in this work also owes a lot to [16]. [17] also devises an energy-efficient cooperative-computing scheme in which a node can partially or totally offload a computing task to a surrounding idle node acting as a helper node. In the context of Mobile Wireless Sensors Networks (MWSNs), [18] augments this framework by optimally selecting the helper node among a set of N surrounding nodes. In [19], a wireless powered cooperative-computing scheme wherein a user node can offload computations to K helper nodes is described. In [20] authors describe Mobile Device Cloud (MDC), i.e., a framework in which power balancing is performed among a cluster of mobile devices, and empirically optimize the collaboration to maximize the lifetime of the set of devices. Finally, in [21], an energy-efficient and incentive-aware network-assisted (i.e., coordinated by the edge of the network), device-to-device (D2D) collaboration framework is presented.

C. Organization of the paper

Section II starts by describing in details the collaborative computing model and the energy and time consumption models for both local computation and communication between the nodes. Next, Sec. III formulates the problem as an optimization problem and analyses its feasibility. Section IV then reformulates the problem, proves its convexity in this new formulation and leverages Lagrange duality theory to gain some insights on the optimal solution of the problem. Section V benchmarks the performances of the optimal collaborative-computing scheme against various other schemes through numerical experiments. Finally, Sec. VI discusses the results obtained in this work and opportunities for future research.

II. SYSTEM MODEL

This section details the collaborative computing model used in this work, namely Map-Reduce, and quantifies the time and energy consumed by each phase of the collaboration.

Throughout this paper, we assume that there is some central entity (e.g., the AP/BS) having perfect knowledge of the channel state information (CSI) and computing capabilities of all the nodes that is responsible for coordinating the collaboration. This makes our collaborative-computing scheme edge-facilitated (or network-assisted).

A. Collaborative computing model

The tasks are shared between the N nodes according to the Map-Reduce framework [10]. First, we assume that the file w can be arbitrarily divided in N smaller files w_n (one for each node) of size $l_n \in \mathbb{R}_{\geq 0}$ bits¹ such that $w_i \cap w_j = \emptyset$ for all $i \neq j$ and $w = \bigcup_{n=1}^N w_n$. We thus have

$$\sum_{n=1}^N l_n = L. \quad (1)$$

As opposed to previous works focusing on CDC [12]–[15], we are thus not assuming any redundancy in the computing loads assigned to each node. Also, the computing load assigned to each node is optimized for energy-efficiency taking into account the heterogeneity of the set of nodes instead of being uniform and fixed ahead of time. In this low-power devices context, we also assume that the downlink rates are much larger than the uplink rates and neglect the time and energy needed to transmit w_n from the AP to node n , for all $n \in [N]$.

To make collaboration between the nodes possible, we also assume that the local data $\{d_n\}_{n=1}^N$ were shared between all the nodes through the AP in a prior phase that we neglect in this work because D is assumed to be relatively small.

During the first phase of the Map-Reduce framework, namely the *Map phase*, each node n computes intermediate values

$$v_{n,m} = g_n(d_m, w_n), \quad m \in [N]$$

where $g_n : [0, 1]^D \times [0, 1]^{l_n} \rightarrow [0, 1]^{(l_n/L)T}$ is the *Map function* executed at node n . The size (in bits) of the intermediate values produced at node n is assumed to be proportional to the computing load assigned to node n , i.e., l_n . Each node n thus computes intermediate values for all the other nodes (i.e., $v_{n,m}$ for all $m \neq n$) and for itself (i.e., $v_{n,n}$) using the part w_n of w received from the AP.

Next, the nodes exchange intermediate values with each other in the so-called *Shuffle phase*. In the absence of a reliable model for the energy consumption of coding operations and for the sake of tractability in order to lay out the foundations of the proposed collaborative-computing framework, coded Shuffling (i.e., CDC [12]–[15]) is not considered in this work. In this simplified Shuffle phase, each node n transmits the intermediate values $v_{n,m} = g_n(d_m, w_n)$ to node m via

¹In practice, l_n should be an integer multiple of the size of the smallest possible division of w . In this work, we relax this practical consideration to avoid dealing with integer programming later on. Note that $l_n = 0$ is also possible, in which case node n does not participate to the collaboration.

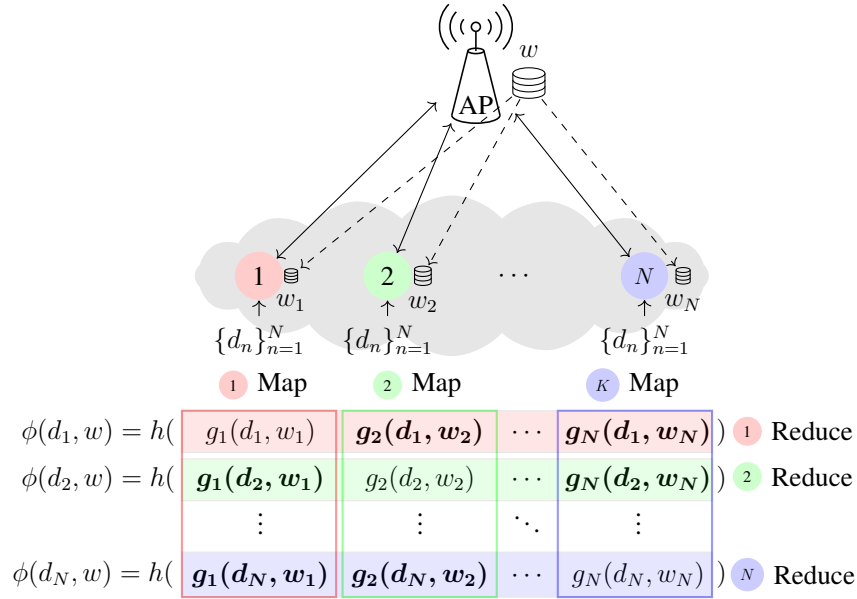


Fig. 1. Illustration of the the Map-Reduce collaborative-computing model. The computation of $\{\phi(d_n, w)\}_{n=1}^N$ is distributed between N nodes. During the Map phase, each node n computes intermediate values $\{g_n(d_m, w_n)\}_{m=1}^N$ (see framed columns above). Next, during the Shuffle phase, the intermediate values in bold on the figure are transmitted via the AP to the nodes for which they have been computed. The AP is said to facilitate the collaboration. Finally, during the Reduce phase, each node m combines the intermediate values $\{g_n(d_m, w_n)\}_{n=1}^N$ to obtain $\phi(d_m, w)$ (see colored rows above).

the AP, for all $m \neq n$. Node n thus needs to transmit $(N - 1)(l_n/L)T$ bits of intermediate values to the AP. To ease notations in the rest of the paper, we define $\alpha = (N - 1)T/L$ as the ratio of the number of bits to be sent to the AP in the Shuffle phase to the number of bits l_n processed during the Map phase. The Map phase can thus be seen as a data compression phase, reducing the size of w_n from l_n bits to αl_n bits of intermediate values before transmission in the Shuffle phase.

Finally, during the *Reduce phase*, each node m combines a total of T bits of intermediate values $\{v_{n,m} = g_n(d_m, w_n)\}_{n=1}^N$ produced by all the collaborating nodes as

$$\phi(d_m, w) = h(g_1(d_m, w_1), g_2(d_m, w_2), \dots, g_N(d_m, w_N))$$

where $h : [0, 1]^T \rightarrow [0, 1]^O$ is the *Reduce function*. The Map-Reduce collaborative computing model is illustrated in Fig. 1.

We note t_n^{MAP} , t_n^{SHU} and t_n^{RED} the amount of time needed for the Map, Shuffle and Reduce phases at node n . Because the Map and Shuffle phases must be over at every node before the

Reduce phase starts (as all the intermediate values need to be available), we have the following constraint

$$t_n^{\text{MAP}} + t_n^{\text{SHU}} \leq \tau - \max_n \{t_n^{\text{RED}}\}, \quad n \in [N]. \quad (2)$$

B. Local computing model

During the Map phase, each node receives l_n bits to process. The number of CPU cycles needed to process one bit of input data at node n is assumed to be given by a constant c_n . At the opposite of our previous work [11], nodes are now assumed to be able to perform dynamic frequency scaling (DFS), i.e., a node can adjust its CPU frequency on the fly depending on the needs. Then, noting κ_n the effective capacitance coefficient (that depends on the chip architecture of each node), the energy needed for computation during the Map phase can be modeled as [6], [7], [16]

$$E_n^{\text{MAP}} = \frac{\kappa_n c_n^3 l_n^3}{(t_n^{\text{MAP}})^2}, \quad n \in [N] \quad (3)$$

with the following constraint

$$c_n l_n \leq t_n^{\text{MAP}} f_n^{\text{max}}, \quad n \in [N] \quad (4)$$

where f_n^{max} is the maximum CPU frequency of node n . Motivated by the fact that $D \ll L$ and to avoid integer variables in our optimization problem later on, the energy and time needed to process the ND bits of shared local data during the Map phase have been neglected in both (3) and (4).

Similarly, the energy needed at node n to combine the T bits of intermediate values during the Reduce phase is modeled as

$$E_n^{\text{RED}} = \frac{\kappa_n c_n^3 T^3}{(t_n^{\text{RED}})^2}, \quad n \in [N] \quad (5)$$

with the following constraint

$$c_n T \leq t_n^{\text{RED}} f_n^{\text{max}}, \quad n \in [N]. \quad (6)$$

Because increasing t_n^{RED} is always favorable for energy-efficiency and because the Reduce phase cannot start before the Map and Shuffle phases are over, one can see that we will always have the same $t_n^{\text{RED}} = t^{\text{RED}}$ across all N nodes. As a consequence, constraint (6) becomes

$$T \max_n \left\{ \frac{c_n}{f_n^{\text{max}}} \right\} \leq t^{\text{RED}} \quad (7)$$

while constraint (2) becomes

$$t_n^{\text{MAP}} + t_n^{\text{SHU}} \leq \tau - t^{\text{RED}}, \quad n \in [N]. \quad (8)$$

C. Communications from the nodes to the AP

During the Shuffle phase, nodes exchange intermediate values through the AP. This exchange thus involves both an uplink communication (nodes to AP) and a downlink communication (AP to nodes). In most applications however, it is reasonable to assume that the downlink rates are much larger than the uplink rates. For this reason, and because we are primarily interested by the energy consumed by the low-power nodes, we neglect the time needed for the downlink communications in this work.

We assume that all the nodes can communicate in an orthogonal manner to the AP (e.g., through frequency division multiple access techniques). We also make the common assumption that the allowed latency τ is smaller than the channel coherence time. Let $h_n \in \mathbb{C}$ denote the wireless channel gain from node n to the AP, p_n the RF transmit power of node n , B the communication bandwidth and N_0 the noise power spectral density at the AP. The achievable uplink rate of node n (in nats/second) is then given by²

$$r_n(p_n) = B \ln\left(1 + \frac{p_n h_n}{N_0 B}\right).$$

Noting P_n^c the constant energy consumption used by the communication circuits at node n , the energy consumed during the Shuffle phase is thus given by

$$E_n^{\text{SHU}} = t_n^{\text{SHU}}(p_n + P_n^c) \quad (9)$$

with the following constraints

$$\alpha l_n \leq t_n^{\text{SHU}} r_n(p_n), \quad n \in [N] \quad (10)$$

and

$$p_n \leq p_n^{\max}, \quad n \in [N] \quad (11)$$

where p_n^{\max} is the maximum RF transmit power at node n .

²The noise power $N_0 B$ can be replaced by $\Gamma N_0 B$, with Γ the SNR gap, to account for practical modulation and coding schemes. This additional factor is left out here for the sake of clarity.

III. PROBLEM FORMULATION

Putting everything together, the energy-efficient wireless collaborative-computing problem can be written as follows

$$\begin{aligned}
 \text{(P1)} : \quad & \underset{l, t^{\text{MAP}}, t^{\text{SHU}}, t^{\text{RED}}, p}{\text{minimize}} \quad \sum_{n=1}^N E_n^{\text{MAP}} + E_n^{\text{SHU}} + E_n^{\text{RED}} \\
 & \text{subject to} \quad (1), (4), (7), (8), (10), (11) \\
 & \quad \quad \quad l_n, t_n^{\text{MAP}}, t_n^{\text{SHU}}, p_n, t^{\text{RED}} \geq 0, \quad n \in [N]
 \end{aligned}$$

where $l, t^{\text{MAP}}, t^{\text{SHU}}$ and p are N -length vectors containing the corresponding variables. Interestingly, this problem can be reformulated as follows: how can we send a total of L bits at a given rate of L/τ bits/second through N parallel special channels consisting of a “computing channel” in series with a wireless communication channel in the most energy-efficient way? This is illustrated in Fig. 2. This interpretation was already mentioned in [17] for a single channel (i.e., for $N = 1$) and is here generalized for multiple parallel channels.

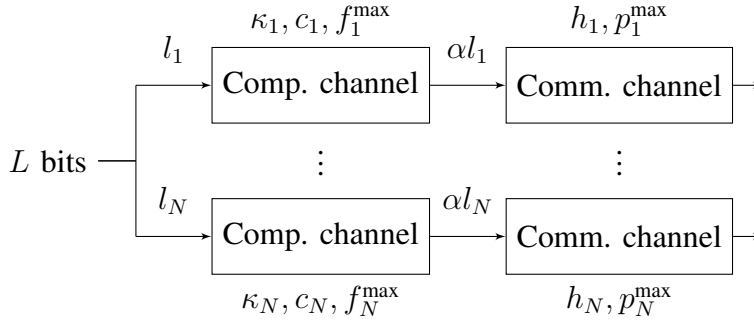


Fig. 2. Another interpretation of the energy-efficient wireless collaborative-computing problem: how can we send a total of L bits at a given rate of L/τ bits/second through N parallel special channels consisting of a “computing channel” in series with a wireless communication channel in the most energy-efficient way?

A. Feasibility

Before solving Problem (P1), we first seek to determine its feasibility condition, i.e., condition that ensures that the system is able to meet the deadline.

Lemma 1 (Feasibility). *Problem (P1) is feasible if and only if the task size L satisfies*

$$L \leq L_{\max} = \sum_{n=1}^N \frac{\tau - T \max_n \left\{ \frac{c_n}{f_n^{\max}} \right\} f_n^{\max}}{1 + \frac{\alpha f_n^{\max}/c_n}{r_n(p_n^{\max})}} \frac{f_n^{\max}}{c_n}.$$

Proof. The maximum computing capacity of the system L_{\max} is obtained by solving the following optimization problem

$$\begin{aligned} L_{\max} &\triangleq \underset{l, t^{\text{MAP}}, t^{\text{SHU}}, t^{\text{RED}}, p}{\text{maximize}} \quad \sum_{n=1}^N l_n \\ &\text{subject to} \quad (4), (7), (8), (10), (11) \\ &\quad l_n, t_n^{\text{MAP}}, t_n^{\text{SHU}}, p_n, t^{\text{RED}} \geq 0 \quad \forall n. \end{aligned}$$

For the maximum computing capacity to be achieved, constraints (8), (11) and (7) must be met, that is, the entire time τ is used by all nodes, all nodes transmit at their maximum RF transmit power p^{\max} and the Reduce phase executes as fast as possible. Next, the two constraints (4) and (10) on l_n can be re-written in a single constraint as follows

$$l_n \leq \min \left\{ \frac{t_n^{\text{MAP}} f_n^{\max}}{c_n}, \frac{1}{\alpha} t_n^{\text{SHU}} r_n(p_n^{\max}) \right\}.$$

At the optimum, this constraint is satisfied and we have

$$\alpha \frac{t_n^{\text{MAP}} f_n^{\max}}{c_n} = t_n^{\text{SHU}} r_n(p_n^{\max})$$

which intuitively means that the number of bits of intermediates values produced by the Map phase at full speed must equal the number of bits that can be transmitted at full speed during the Shuffle phase. Then using

$$t_n^{\text{MAP}} + t_n^{\text{SHU}} = \tau - T \max_n \left\{ \frac{c_n}{f_n^{\max}} \right\},$$

we finally obtain

$$t_n^{\text{MAP}} = \frac{\tau - T \max_n \left\{ \frac{c_n}{f_n^{\max}} \right\}}{1 + \frac{\alpha f_n^{\max}/c_n}{r_n(p_n^{\max})}} \quad (12)$$

and

$$t_n^{\text{SHU}} = \frac{\tau - T \max_n \left\{ \frac{c_n}{f_n^{\max}} \right\}}{1 + \frac{r_n(p_n^{\max})}{\alpha f_n^{\max}/c_n}}. \quad (13)$$

The maximum computing load L_{\max} is thus given by

$$L_{\max} = \sum_{n=1}^N \frac{\tau - T \max_n \left\{ \frac{c_n}{f_n^{\max}} \right\} f_n^{\max}}{1 + \frac{\alpha f_n^{\max}/c_n}{r_n(p_n^{\max})}} \frac{f_n^{\max}}{c_n}.$$

□

We see through (12) and (13) that, at full capacity, the time for the Map and Shuffle phases is shared according to the ratio of (i) the maximum rate at which the Map phase can produce

intermediate values $\alpha f_n^{\max}/c_n$, and (ii) the maximum rate at which the Shuffle phase can transmit intermediate values $r_n(p_n^{\max})$. At lower than full capacity, these time intervals will be able to adjust taking into account the energy-efficiency of both phases.

IV. OPTIMAL SOLUTION

Inspired by [16], we then introduce a new set of variables $E_n = t_n^{\text{SHU}} p_n$, i.e., the RF energy consumed by the Shuffle phase, and substitute p_n for E_n/t_n^{SHU} to convexify Problem (P1). With this new variable, constraints (10) and (11) can be re-written as

$$\alpha l_n \leq t_n^{\text{SHU}} r_n \left(\frac{E_n}{t_n^{\text{SHU}}} \right) \quad (14)$$

and

$$E_n \leq t_n^{\text{SHU}} p_n^{\max} \quad (15)$$

respectively, for all $n \in [N]$. Problem (P1) thus becomes

$$\begin{aligned} \text{(P2)} : \quad & \underset{l, t^{\text{MAP}}, t^{\text{SHU}}, t^{\text{RED}}, E}{\text{minimize}} && \sum_{n=1}^N \frac{\kappa_n c_n^3 l_n^3}{(t_n^{\text{MAP}})^2} + E_n + t_n^{\text{SHU}} P_n^c + \frac{\kappa_n c_n^3 T^3}{(t_n^{\text{RED}})^2} \\ & \text{subject to} && (1), (4), (7), (8), (14), (15) \\ & && l_n, t_n^{\text{MAP}}, t_n^{\text{SHU}}, E_n, t_n^{\text{RED}} \geq 0 \quad n \in [N]. \end{aligned}$$

We now prove the convexity of this new formulation.

Lemma 2 (Convexity). *Problem (P2) is convex.*

Proof. As this is a minimization problem, we start by showing the convexity of the objective function. The function x^3 is a convex function for $x \geq 0$. Its perspective function, x^3/y^2 , is thus also a convex function for $y \geq 0$. The term associated to the energy consumed by the Map phase is thus jointly convex with respect to $l_n \geq 0$ and $t_n^{\text{MAP}} > 0$. Next, the terms associated to the energy consumed by the Shuffle phase are linear and hence convex by definition. Finally, the function $1/x^2$ is a convex function with respect to $x > 0$ which makes the term associated to the energy consumed by the Reduce phase a convex function as well. As convexity is preserved under addition, the objective function of Problem (P2) is a convex function. Next, we show that the set defined by the constraints is a convex set. The equality constraint (1) is affine and thus defines a hyperplane. Next, inequalities (4), (7), (8), and (15) are either linear or affine and thus define a polyhedron. The only remaining constraint (omitting trivial positivity constraints on all variables) is then constraint (14). For constraint (14) to define a convex set, its right-hand side

term must be a concave function. The function $r_n(x)$ is a concave function with respect to $x \geq 0$. Its perspective function, $yr_n(x/y)$ is thus also a concave function with respect to $x \geq 0$ and $y > 0$. Because the intersection of a (convex) hyperplane, a (convex) polyhedron and a convex sublevel set remains a convex set, the set defined by the constraints of Problem (P2) is also convex. \square

Problem (P2) can easily be solved using a software for convex optimization like `cvxopt` [22]. This wouldn't however offer any interpretation of the results. To this effect, we seek to gain some insights into the optimal solution to Problem (P2) mathematically using Lagrange duality theory.

We thus let $\lambda \in \mathbb{R}$, $\beta_n \geq 0$, $\mu_n \geq 0$ be the Lagrange multipliers associated with constraints (1), (8) and (14) respectively. The partial Lagrangian is then given by

$$\begin{aligned} \mathcal{L}(\mathbf{x}, \boldsymbol{\mu}, \boldsymbol{\beta}, \lambda) &= \sum_{n=1}^N \frac{\kappa_n c_n^3 l_n^3}{(t_n^{\text{MAP}})^2} + E_n + t_n^{\text{SHU}} P_n^c + \frac{\kappa_n c_n^3 T^3}{(t_n^{\text{RED}})^2} \\ &\quad + \sum_{n=1}^N \mu_n \left(\alpha l_n - t_n^{\text{SHU}} r_n \left(\frac{E_n}{t_n^{\text{SHU}}} \right) \right) \\ &\quad + \beta_n (t_n^{\text{MAP}} + t_n^{\text{SHU}} + t_n^{\text{RED}} - \tau) \\ &\quad + \lambda \left(L - \sum_{n=1}^N l_n \right) \end{aligned}$$

where optimization variables and Lagrange multipliers have been aggregated in the corresponding vectors to ease notations. The dual function is then given by

$$\begin{aligned} \text{(DF)} : \quad g(\boldsymbol{\mu}, \boldsymbol{\beta}, \lambda) &= \min_{\mathbf{x}} \quad \mathcal{L}(\mathbf{x}, \boldsymbol{\mu}, \boldsymbol{\beta}, \lambda) \\ &\text{s.t.} \quad (4), (7), (15) \\ &\quad 0 \leq t_n^{\text{MAP}}, t_n^{\text{SHU}}, t_n^{\text{RED}} \leq \tau \quad n \in [N], \\ &\quad l_n, E_n \geq 0 \quad n \in [N]. \end{aligned}$$

As the dual function provides a lower bound to the optimal value of the primal problem, we then seek to maximize it to obtain the best possible lower bound. The dual problem is given by

$$\begin{aligned} \text{(D1)} : \quad &\underset{\boldsymbol{\mu}, \boldsymbol{\beta}, \lambda}{\text{maximize}} \quad g(\boldsymbol{\mu}, \boldsymbol{\beta}, \lambda) \\ &\text{subject to} \quad \mu_n, \beta_n \geq 0, \quad n \in [N]. \end{aligned}$$

Problem (P2) is convex (Lemma 2) and satisfies Slater's condition if it is strictly feasible (in the sense given in Lemma 1). Strong duality thus holds and Problem (P2) can be solved by solving the dual problem (D1).

A. Derivation of the dual function

Before solving the dual problem (D1), we seek to evaluate the dual function $g(\boldsymbol{\mu}, \boldsymbol{\beta}, \boldsymbol{\lambda})$ for all $\boldsymbol{\mu}, \boldsymbol{\beta}, \boldsymbol{\lambda}$ by solving Problem (DF). To this effect, we first decompose Problem (DF) in $2N + 1$ sub-problems as follows

$$\begin{aligned} & \underset{l_n, t_n^{\text{MAP}}}{\text{minimize}} && \frac{\kappa_n c_n^3 l_n^3}{(t_n^{\text{MAP}})^2} + (\alpha \mu_n - \lambda) l_n + \beta_n t_n^{\text{MAP}} \\ & \text{subject to} && 0 \leq l_n \leq t_n^{\text{MAP}} f_n^{\text{max}} / c_n \\ & && t_n^{\text{MAP}} \leq \tau \end{aligned} \quad (16)$$

$$\begin{aligned} & \underset{E_n, t_n^{\text{SHU}}}{\text{minimize}} && E_n + (P_n^c + \beta_n) t_n^{\text{SHU}} - \mu_n t_n^{\text{SHU}} r_n \left(\frac{E_n}{t_n^{\text{SHU}}} \right) \\ & \text{subject to} && 0 \leq E_n \leq t_n^{\text{SHU}} p_n^{\text{max}} \\ & && t_n^{\text{SHU}} \leq \tau \end{aligned} \quad (17)$$

$$\begin{aligned} & \underset{t^{\text{RED}}}{\text{minimize}} && \sum_{n=1}^N \frac{\kappa_n c_n^3 T^3}{(t^{\text{RED}})^2} + \beta_n t^{\text{RED}} \\ & \text{subject to} && \max_n \left\{ \frac{c_n T}{f_n^{\text{max}}} \right\} \leq t^{\text{RED}} \leq \tau. \end{aligned} \quad (18)$$

It is interesting to note that Problems (16) and (17) correspond to the Map and Shuffle phases at node n respectively while Problem (18) corresponds to the Reduce phase.

Lemma 3 (Solution of Problem (16)). *For any $\mu_n, \beta_n \geq 0$ and $\lambda \in \mathbb{R}$, the optimal solution of Problem (16) satisfies*

$$l_n^* = M_n^* t_n^{\text{MAP}*} \quad (19)$$

with M_n^* , the effective processing rate (in bits/second) of node n defined as

$$M_n^* \triangleq \begin{cases} 0 & \lambda - \alpha \mu_n \leq 0 \\ \sqrt{\frac{\lambda - \alpha \mu_n}{3 \kappa_n c_n^3}} & \lambda - \alpha \mu_n \in]0, 3 \kappa_n c_n (f_n^{\text{max}})^2[\\ \frac{f_n^{\text{max}}}{c_n} & \lambda - \alpha \mu_n \geq 3 \kappa_n c_n (f_n^{\text{max}})^2 \end{cases} \quad (20)$$

and $t_n^{\text{MAP}*}$ given by

$$t_n^{\text{MAP}*} \begin{cases} = 0 & \rho_{1,n} < 0 \\ \in [0, \tau] & \rho_{1,n} = 0 \\ = \tau & \rho_{1,n} > 0 \end{cases} \quad (21)$$

with $\rho_{1,n} = 2\kappa_n(c_n M_n^*)^3 - \beta_n + \gamma_{2,n} \frac{f_n^{\max}}{c_n}$ and

$$\gamma_{2,n} = \begin{cases} 0 & M_n^* < \frac{f_n^{\max}}{c_n} \\ \lambda - \alpha\mu_n - 3\kappa_n c_n (f_n^{\max})^2 & M_n^* = \frac{f_n^{\max}}{c_n}. \end{cases} \quad (22)$$

Proof. See Appendix A. □

Lemma 4 (Solution of problem (17)). *For any $\mu_n, \beta_n \geq 0$, the optimal solution of Problem (17) satisfies*

$$E_n^* = p_n^* t_n^{SHU^*} \quad (23)$$

with p_n^* , the RF transmit power used during the Shuffle phase at node n defined as

$$p_n^* \triangleq \begin{cases} 0 & B\mu_n \leq \frac{BN_0}{h_n} \\ B\left(\mu_n - \frac{N_0}{h_n}\right) & B\mu_n \in \left[\frac{BN_0}{h_n}, \frac{BN_0}{h_n} + p_n^{\max}\right] \\ p_n^{\max} & B\mu_n \geq \frac{BN_0}{h_n} + p_n^{\max} \end{cases} \quad (24)$$

and $t_n^{SHU^*}$ given by

$$t_n^{SHU^*} \begin{cases} = 0 & \rho_{2,n} < 0 \\ \in [0, \tau] & \rho_{2,n} = 0 \\ = \tau & \rho_{2,n} > 0 \end{cases} \quad (25)$$

with $\rho_{2,n} = \mu_n r_n(p_n^*) - P_n^c - \beta_n - \mu_n \frac{p_n^* \frac{h_n}{N_0}}{1 + p_n^* \frac{h_n}{N_0 B}} + \delta_{2,n} p_n^{\max}$ and

$$\delta_{2,n} = \begin{cases} 0 & p_n^* < p_n^{\max} \\ \mu_n \frac{\frac{h_n}{N_0}}{1 + p_n^{\max} \frac{h_n}{N_0 B}} - 1 & p_n^* = p_n^{\max}. \end{cases} \quad (26)$$

Proof. See Appendix B. □

Lemma 5 (Solution of Problem (18)). *For any $\beta_1, \dots, \beta_N \geq 0$, the optimal solution of Problem (18) satisfies*

$$t^{RED^*} = \begin{cases} T \max_n \left\{ \frac{c_n}{f_n^{\max}} \right\} & \sum_{n=1}^N \beta_n > \frac{2 \sum_{n=1}^N \kappa_n c_n^3}{\left(\max_n \left\{ \frac{c_n}{f_n^{\max}} \right\} \right)^3} \\ T \sqrt[3]{\frac{2 \sum_{n=1}^N \kappa_n c_n^3}{\sum_{n=1}^N \beta_n}} & \sum_{n=1}^N \beta_n \leq \frac{2 \sum_{n=1}^N \kappa_n c_n^3}{\left(\max_n \left\{ \frac{c_n}{f_n^{\max}} \right\} \right)^3}. \end{cases} \quad (27)$$

Proof. See Appendix C. □

B. Maximization of the dual function and interpretation

The dual function being concave but non-differentiable, we could now maximize it using the subgradient-based ellipsoid method, as was done for example in [16]. However, in addition to being unpractical to solve the actual problem (when compared to the use of a convex optimization solver like `cvxopt` [22]), this method doesn't offer any additional insight into the structure of the optimal solution.

Instead, we intuitively look at what happens if we maximize the dual function $g(\boldsymbol{\mu}, \boldsymbol{\beta}, \lambda)$ taking into account the results of Lemmas 3, 4 and 5. To ease the analysis, we start with $\lambda = 0$ and $\mu_n = 0$ for all n . In this case, $l_n^* = 0$ for all nodes and the penalty term $L - \sum_{n=1}^N l_n^* = L$ associated with λ appearing in the dual function is strictly positive. Intuitively, this implies that the task has not be fully distributed across the nodes, violating constraint (1). It is thus possible to increase the value of the dual function through this positive penalty term by increasing the value of λ . Because l_n^* is proportional to $\sqrt{\lambda - \alpha\mu_n}$ through M_n^* , this increases the number of bits l_n^* processed by each node. Moreover, because l_n^* is also inversely proportional to $\sqrt{\kappa_n c_n^3}$ through M_n^* , less energy-efficient nodes (i.e., the ones with larger values of $\kappa_n c_n^3$) get fewer bits to process. The value of λ can be increased in this way until the penalty term $L - \sum_{n=1}^N l_n^*$ equals 0 (i.e., until the task is fully distributed across the nodes). Next, because $\mu_n = 0$ for all nodes as of now, the penalty term $\alpha l_n^* - t_n^{\text{SHU}^*} r_n(p_n^*) = \alpha l_n^*$ associated with μ_n appearing in the dual function is strictly positive for all nodes. Intuitively, this implies that the rate constraint (14) is violated for all nodes. It is thus possible to increase the value of the dual function through this penalty term by increasing the value of μ_n . Increasing μ_n has a double effect: (i) it decreases the value of l_n^* because l_n^* is proportional to $\sqrt{\lambda - \alpha\mu_n}$, and (ii) it increases the value of p_n^* because p_n^* is directly proportional to μ_n . Combined, these two effects work together towards satisfying the rate constraint (14). For nodes with very bad channel or very low maximum RF transmit power p_n^{\max} , μ_n could increase so much that $\lambda - \alpha\mu_n$ would become negative, meaning that the number of bits to be processed l_n^* would fall to 0. At this point, there is an iterative interplay between λ and $\{\mu_n\}_{n=1}^N$ in which both successively increase to maximize the dual function until both constraints (1) and (14) are satisfied and a maximum has been reached.

It is now possible to give a waterfilling-like interpretation of the structure of the optimal computing load partition $\{l_n^*\}_{n=1}^N$. First, λ acts as a kind of global (i.e., across all nodes) water level for $\{l_n^*\}_{n=1}^N$ through the effective processing rate M_n^* . Then, $\alpha\mu_n$ can be seen as the base of

the water vessel of node n . Following the above discussion, this base $\alpha\mu_n$ mainly depends on the communication capabilities of node n (i.e., h_n and p_n^{\max}). Finally, the actual water content of each vessel, i.e., $\lambda - \alpha\mu_n$ is divided by $3\kappa_n c_n^3$. This term, related to the computing energy-efficiency of node n can be interpreted as a pressure applied to the water vessel of each node. The less energy-efficient node n is, the bigger $3\kappa_n c_n^3$ becomes and the more pressure is applied to its water vessel.

V. NUMERICAL RESULTS

In this section, the performances of the optimal collaborative-computing scheme (denoted Opt in what follows) are benchmarked against various other schemes through numerical experiments. The schemes used for comparison are

- **Blind**: the task allocation (i.e., choosing the value of l_n for each node n) doesn't take into account the heterogeneity of the nodes; the scheme is blind to node diversity (both in term of computing and communicating capabilities). In this case, the variable l_n is set to L/N for each node n . This corresponds to what is done in most works on CDC assuming homogeneous nodes [12]–[15].
- **NoDFS**: the CPU frequency of each node n is fixed to its maximum value f_n^{\max} rather than being optimized for energy-efficiency. In this case, the variable t_n^{MAP} is set to $c_n l_n / f_n^{\max}$ for each node n while t_n^{RED} (now different for each node) is set to $c_n T / f_n^{\max}$. This scheme is close to the one proposed in our previous work [11].
- **Blind-NoDFS**: this scheme combines the two previous cases. In this case, $l_n = L/N$ and $t_n^{\text{MAP}} = \frac{c_n}{f_n^{\max}} \frac{L}{N}$ for each node n while $t_n^{\text{RED}} = c_n T / f_n^{\max}$. The only optimization left here concerns the Shuffle phase and the variables t_n^{SHU} and E_n .
- **NoOpt**: in this scheme, nothing is optimized. This is basically **Blind-NoDFS** with $\alpha \frac{L}{N} = t_n^{\text{SHU}} r_n \left(\frac{E_n}{t_n^{\text{SHU}}} \right)$ and $E_n = t_n^{\text{SHU}} p_n^{\max}$.

Unless stated otherwise, the parameters used in the following numerical experiments are given in Table I [6], [7], [16].

A. Maximum computation load and outage probability

To show that the proposed scheme indeed enhances the computing capabilities of individual nodes, we start by comparing the maximum computation load of Opt and **Blind**, noted

TABLE I
PARAMETERS USED IN THE NUMERICAL EXPERIMENTS.

Parameter	Value	Units
κ_n	$\overset{\text{i.i.d.}}{\sim} \text{Unif}([10^{-28}, 10^{-27}])$	/
c_n	$\overset{\text{i.i.d.}}{\sim} \text{Unif}([500, 1500])$	[CPU cycles/bit]
f_n^{\max}	$\overset{\text{i.i.d.}}{\sim} \text{Unif}([1, 3])$	[GHz]
h_n	$\overset{\text{i.i.d.}}{\sim} \mathcal{CN}(0, 10^{-3})$ (Rayleigh fading)	/
p_n^{\max}	$\overset{\text{i.i.d.}}{\sim} \text{Unif}([10, 25])$	[mW]
P_n^c	$\overset{\text{i.i.d.}}{\sim} \text{Unif}([10, 25])$	[mW]
B	15	[kHz]
N_0	1	[nW/Hz]

L_{\max}^{Opt} and L_{\max}^{Blind} , respectively. Other schemes are not included here as $L_{\max}^{\text{NoDFS}} = L_{\max}^{\text{Opt}}$ and $L_{\max}^{\text{Blind-NoDFS}} = L_{\max}^{\text{Blind}} = L_{\max}^{\text{NoOpt}}$.

For Opt , the maximum computation load L_{\max}^{Opt} can be readily obtained using Lemma 1. For Blind , we introduce the following Lemma.

Lemma 6 (Maximum computing load of Blind). *The maximum computing load achievable by the Blind scheme is given by*

$$L_{\max}^{\text{Blind}} = N \min \left\{ \frac{\tau - T \max_n \left\{ \frac{c_n}{f_n^{\max}} \right\} f_n^{\max}}{1 + \frac{\alpha f_n^{\max}/c_n}{r_n(p_n^{\max})}} \frac{f_n^{\max}}{c_n} \right\}.$$

Proof. Obtaining L_{\max}^{Blind} requires solving the following linear program (LP)

$$\begin{aligned} L_{\max}^{\text{Blind}} &\triangleq \underset{l, t^{\text{MAP}}, t^{\text{SHU}}}{\text{maximize}} && Nl \\ \text{subject to} &&& c_n l \leq t_n^{\text{MAP}} f_n^{\max} && \forall n \\ &&& \alpha l \leq t_n^{\text{SHU}} r_n(p_n^{\max}) && \forall n \\ &&& t^{\text{RED}} \geq T \max_n \left\{ \frac{c_n}{f_n^{\max}} \right\} \\ &&& t_n^{\text{MAP}} + t_n^{\text{SHU}} \leq \tau - t^{\text{RED}} && \forall n \\ &&& l, t_n^{\text{MAP}}, t_n^{\text{SHU}} \geq 0 && \forall n \end{aligned}$$

A reasoning quite similar to the one used in Lemma 1 – and omitted here for the sake of space – can then be used to obtain the analytical expression given above. \square

Values of L_{\max}^{Opt} and L_{\max}^{Blind} for different values of the allowed latency τ and various number of nodes N are plotted in Fig. 3. As expected, both L_{\max}^{Opt} and L_{\max}^{Blind} grow with the allowed latency τ . However, L_{\max}^{Opt} grows with τ much faster than L_{\max}^{Blind} does. Next, one can see that increasing the number of nodes N for a given allowed latency τ is always more profitable for `Opt` than for `Blind`. Furthermore, the benefits of further increasing the number of nodes N remain constant for `Opt` but quickly saturates for `Blind`. Both observations can be explained by the fact that `Opt` is able to leverage nodes diversity by optimally exploiting the different computing and communicating capabilities of the nodes while `Blind`, as per its name, is not.

Another way of looking at the maximum computation loads of the different schemes is through what we define as the ‘‘outage probability’’ of the system. In this context, the outage probability is defined, for a random heterogeneous set of nodes and a given allowed latency τ , as the probability that the maximum computing load that can be processed by the system is lower than the actual computing L , i.e.,

$$P_{\text{out}}^* = \Pr [L \geq L_{\max}^*].$$

For a given task size L , this probability can be empirically computed by averaging over a large number of randomly generated sets of nodes. For $L = 10 \text{ Mb}$, both $P_{\text{out}}^{\text{Opt}}$ and $P_{\text{out}}^{\text{Blind}}$ are depicted in Fig. 4 as a function of the allowed latency τ and for multiple number of nodes N . This plot again demonstrates the benefits of leveraging nodes diversity to distribute the task among the nodes. At the opposite, we see that `Blind` suffers from node diversity. Indeed, for larger values of the allowed latency τ , increasing the number of nodes N penalizes `Blind` by increasing its outage probability $P_{\text{out}}^{\text{Blind}}$. Intuitively, this again comes from the fact that increasing the number of nodes N increases the probability of having a very weak node limiting the whole system. Mathematically, the lower tail of the distribution of L_{\max}^{Blind} grows larger and larger with N , making the distribution more and more skewed towards small values of L_{\max}^{Blind} . This also explains why this trend was not visible on Fig. 3 as it only shows the mean of the distribution of L_{\max}^{Blind} . In addition, it appears that the benefits on $P_{\text{out}}^{\text{Blind}}$ of allowing a looser deadline (for a given N) saturate as the value of τ increases beyond a certain point that varies with the number of nodes N . Again, and for the same reason, this trend was not visible on Fig. 3 and cannot be explained by looking at the mean of L_{\max}^{Blind} only. This saturation effect appears when the mode of the distribution of L_{\max}^{Blind} becomes larger than the value of the actual computing load L used to compute $P_{\text{out}}^{\text{Blind}}$. Passed this point, the benefits on $P_{\text{out}}^{\text{Blind}}$ of further pushing the mode to larger values by increasing τ

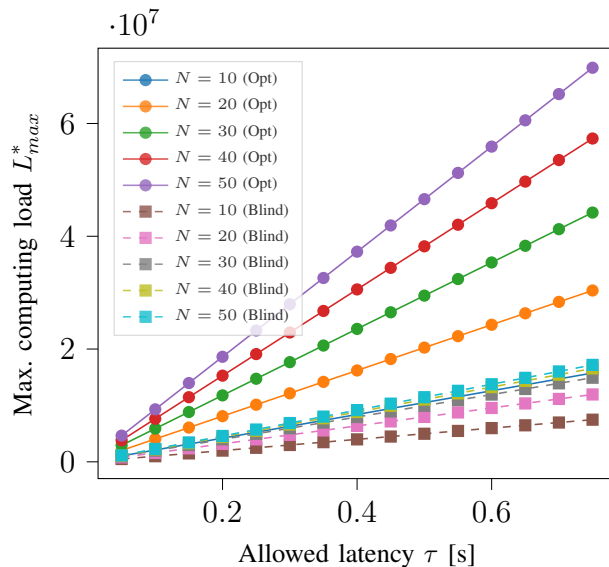


Fig. 3. Maximum computation loads L_{max}^{Opt} and L_{max}^{Blind} averaged over 1.000.000 random instances of the problem. Note that L_{max}^{Opt} for $N = 10$ is hidden by L_{max}^{Blind} for $N = 30, 40$ and 50 .

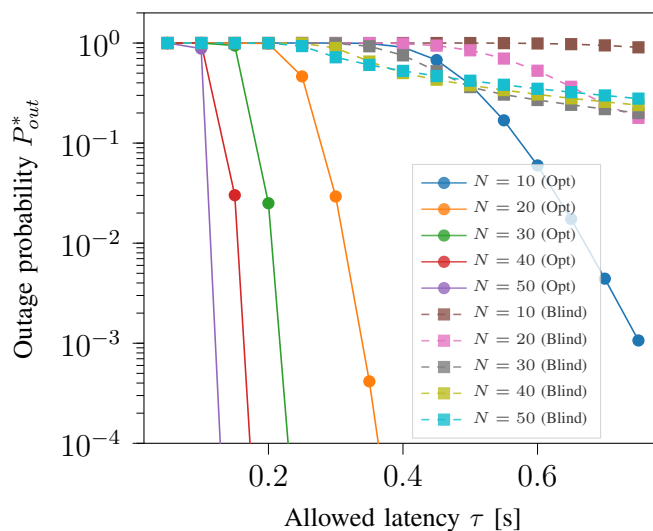


Fig. 4. Empirical outage probability P_{out}^{Opt} and P_{out}^{Blind} for $L = 10$ Mb, averaged over 1.000.000 random instances of the problem.

become smaller and smaller.

B. Energy consumption

We now look at the energy consumed by the different collaborative-computing schemes. Fig. 5a depicts the total energy consumed per bit processed for different numbers of nodes

N , while Fig. 5b depicts the energy consumed by each phase of the collaboration (i.e., Map, Shuffle and Reduce). First, one can observe that the energy consumed by both `Blind-NoDFS` and `NoOpt` is actually the same. This stems from the fact that it is always optimal (from an energy-efficiency point of view) for constraint (14) to be met. Indeed, the opposite would mean that the node is investing either too much time t_n^{SHU} (hence increasing the energy consumption of the communications circuits $t_n^{\text{SHU}} P_n^c$) or too much RF energy E_n with regards to the number of bits αl_n that needs to be transmitted in the Shuffle phase. For the same reason, constraint (15) is almost always satisfied as well, meaning that nodes participating to the Shuffle phase transmit at the maximum RF power allowed, i.e., p_n^{max} . Schemes `Blind-NoDFS` and `NoOpt` are thus equivalent and both transmit at the maximum RF transmit power and at the maximum rate. These two observations are valid for all the other schemes as well. In addition, the energy per bit consumed by both `Blind-NoDFS` and `NoOpt` is roughly constant with the number of nodes. At the opposite, the energy consumed by the other schemes decreases with N as diversity across the nodes is exploited for energy-efficiency. Interestingly, optimizing $\{t_n^{\text{MAP}}\}_{n=1}^N$ and t^{RED} only (in `Blind`) is more beneficial than optimizing l_n only (in `NoDFS`), even though the number of bits assigned to each node for processing by `Blind` is uniform across the nodes, and thus blind to diversity. Combining both schemes in `Opt` leads to a gain in energy-efficiency with respect to `NoOpt` reaching two orders of magnitude for large values of N .

Fig. 5b breaks down the energy consumption of the different schemes in 3 components: E^{MAP} , E^{SHU} and E^{RED} . Note that `NoOpt`, being equivalent to `Blind-NoDFS`, has been omitted to avoid cluttering the plot. First, it appears that the energy consumption of the Map phase largely dominates the energy consumption of the Shuffle and Reduce phases for small values of N^3 . As the number of nodes N increases, this difference decreases for all schemes leveraging diversity across the nodes (i.e., all but `Blind-NoDFS`). At the opposite, the energy consumed by the Shuffle phase increases with the number of nodes N , no matter the scheme used. This figure also shows that there is not much (if anything) to gain from optimization in the Shuffle phase. Next, one can see that the energy efficiency of the Reduce phase increases with N when t^{RED} can be optimized (i.e., when nodes can perform DFS). This decrease with N is however slower than

³Note that this statement is strongly dependent on the energy consumption model and the parameters used for the numerical experiments. As an example, increasing the number of bits transmitted during the Shuffle phase, αl_n , through the size of the intermediate values T would directly result in an increase of E^{SHU} by the same factor.

what we observed for the Map phase. For `Blind`, this can be explained by the fact that priority in the optimization is given to the more energy intensive Map phase. For `Opt`, this comes from the fact that, at the opposite of the Map phase, all nodes have to perform the Reduce phase. Finally, for `NoDFS` and `Blind-NoDFS`, each node has to perform the Reduce phase at full speed causing E^{RED} to increase with N .

C. Energy-latency trade-off

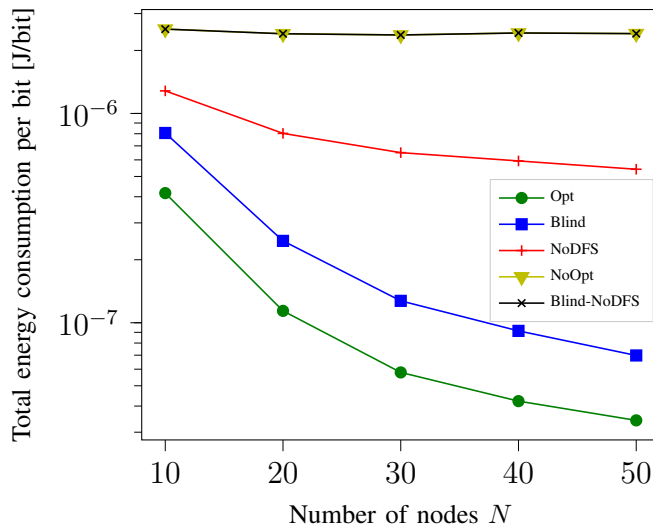
Fig. 6 depicts the total energy consumption per bit and the energy consumed per bit by each phase for the different schemes and for different values of the allowed latency τ . Interestingly, Fig. 6 closely resembles Fig. 5, implying that the effect of increasing the number of nodes N is roughly equivalent to the effect of increasing the allowed latency τ . The underlying mechanisms, however, are different. For schemes where nodes are able to perform DFS (i.e., `Opt` and `Blind`), increasing τ enables the nodes to further decrease their CPU frequency, hence saving energy. For `NoDFS`, increasing τ enables the system to increase the number of bits assigned to the most energy-efficient nodes, hence reducing the load on less energy-efficient nodes and again saving energy.

D. Number of participating nodes

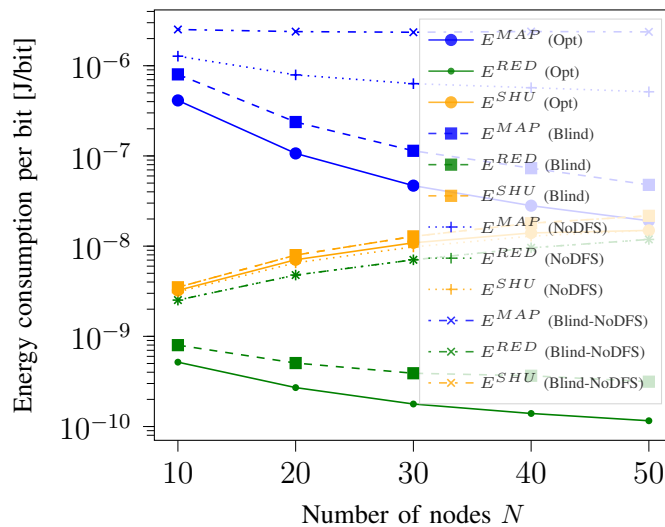
Finally, Fig. 7 shows the average fraction of nodes participating to the collaboration, i.e., nodes with $l_n > 0$ that thus participate to the Map and Shuffle phases, as a function of the computation load L/L_{max} . For `Blind` (and `Blind-NoDFS`), this fraction is of course constant and equal to 1 as $l_n = L/N$ for all n . For `Opt`, this fraction starts at around 0.6 for very small computing loads and quickly reaches 1 for computing loads > 0.2 . At the opposite, for `NoDFS`, the fraction of nodes participating to the Map and Shuffles phases closely follows the fraction L/L_{max} . To explain these radically different behaviors, we look at the energy consumed by the Map phase at each node n for both schemes. For `Opt` first, Eq. (3) indicates that E_n^{MAP} is a cubic function of l_n . For `NoDFS`, injecting $t_n^{\text{MAP}} = c_n l_n / f_n^{\text{max}}$ in (3) shows that E_n^{MAP} becomes a linear function of l_n . This explains why the computing load is more evenly spread across nodes for `Opt` than for `NoDFS`.

VI. DISCUSSION AND FUTURE WORKS

This work built upon our previous work [11] to further highlight the benefits of leveraging devices diversity – whether in term of computation or communication capabilities – to enhance



(a) Comparison of the total energy consumed by the different schemes as a function of the number of nodes N . Note that the energy consumption is the same for both NoOpt (yellow curve) and Blind-NoDFS (black curve).



(b) Breakdown of the energy consumed by the three phases of the collaboration as a function of the number of nodes N . Note that the energy consumption for the Reduce phase is the same for both NoDFS and Blind-NoDFS.

Fig. 5. Energy consumption of the nodes for $L = 1$ Mb, $T = 100$ b and $\tau = 100$ ms as a function of the number of nodes N . Each point is the result of an average over 100 feasible (for each scheme) instances of the problem, i.e., instances for which $L \leq L_{\max}^{\text{Opt}}, L_{\max}^{\text{Blind}}$.

individual computing capabilities of the nodes while increasing energy-efficiency of the system as a whole. As mentioned in the introduction, this makes collaborative-computing another potential viable architecture to be used in conjunction with MEC and MCC to enable ubiquitous computing on heterogeneous devices. However, further validation with more realistic communication models is needed. Interferences between nodes, for example, were neglected in this work. As the interference level is expected to increase with the number of nodes participating to the Shuffle phase, taking into account interference in the communication model could have a significant impact on the number of nodes participating to the collaboration. On the other hand, the system could also optimize channel allocation across nodes, which was considered to be given in this work. Optimizing channel (and potentially bandwidth) allocation across nodes would add another degree of freedom in the system, enabling additional energy savings and increased system-wise performance. This would however come at the cost of a complexified optimization problem involving integer variables. Next, the Shuffle phase could also be further optimized by integrating results from Coded Distributed Computing (CDC) [12]–[15]. Correctly modeling the energy-consumption of network coding operations and the resulting communication-computation trade-offs is however quite challenging. Downlink communications were also neglected in this work. While this makes sense in a scenario where optimizing the energy-consumption of end devices is the primary objective, care should be taken to avoid simply moving the energy burden

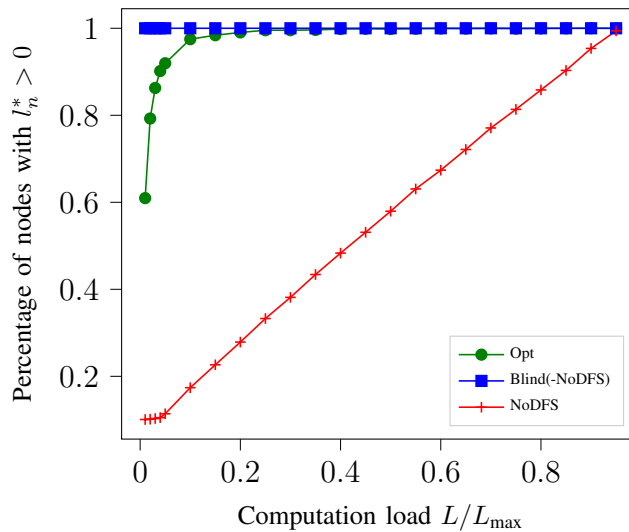
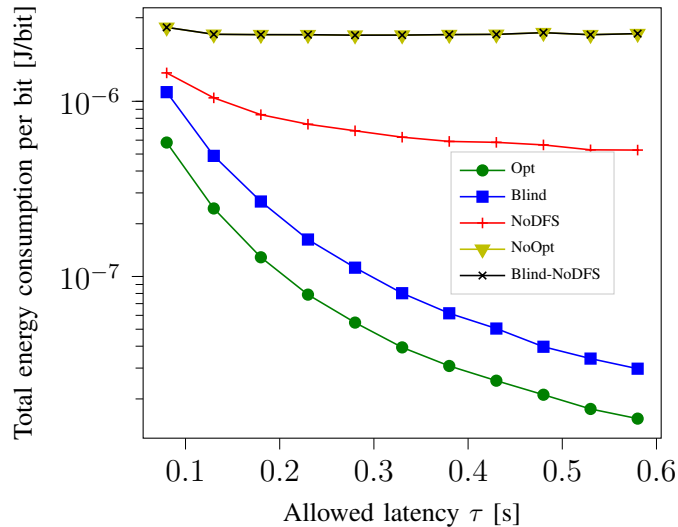
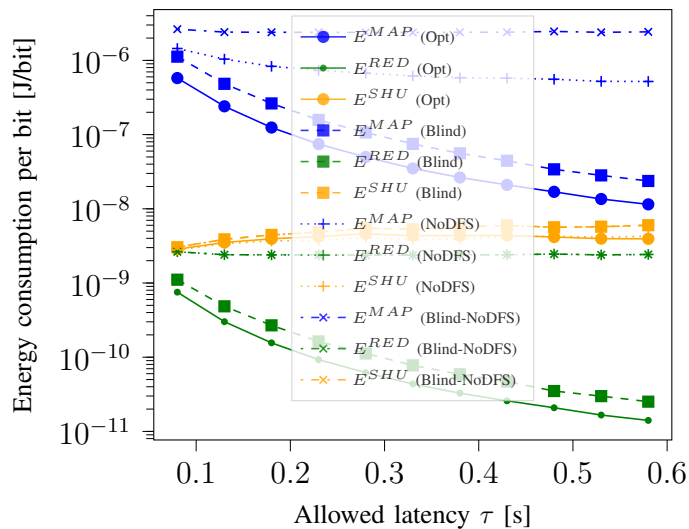


Fig. 7. Average fraction of nodes participating to the collaboration, i.e., nodes with $l_n^* > 0$ that thus participate to the Map and Shuffle phases, as a function of the computing load L/L_{\max} .



(a) Comparison of the total energy consumed by the different schemes as a function of the allowed latency τ . Note that the energy consumption is the same for both NoOpt (yellow curve) and Blind-NoDFS (black curve).



(b) Breakdown of the energy consumed by the three phases of the collaboration as a function of the allowed latency τ . Note that the energy consumption for the Reduce phase is the same for both NoDFS and Blind-NoDFS.

Fig. 6. Energy consumption of the nodes when $L = 1$ Mb, $T = 100$ b and $N = 10$. Each point is the result of an average over 100 feasible (for each scheme) instances of the problem, i.e., instances for which $L \leq L_{\max}^{\text{Opt}}, L_{\max}^{\text{Blind}}$.

to the edge of the network. Finally, it could also be interesting to add the distance between nodes and the AP/BS in the communication model and study the relation between this distance and the computing/communication load assigned to each node.

ACKNOWLEDGMENT

AP is a Research Fellow of the F.R.S.-FNRS. This work was also supported by F.R.S.-FNRS under the EOS program (project 30452698, “MULTI-SERVICE WIRELESS NETWORK”). Authors would also like to thank Emre Kilcioglu for proofreading and comments.

APPENDIX

A. Proof of Lemma 3

Problem (16) being convex, the optimal solution satisfies the KKT conditions. The Lagrangian of problem (16) is given by

$$\begin{aligned} \mathcal{L}_{1,n} = & \frac{\kappa_n c_n^3 l_n^3}{(t_n^{\text{MAP}})^2} + (\alpha \mu_n - \lambda) l_n + \beta_n t_n^{\text{MAP}} - \gamma_{1,n} l_n \\ & + \gamma_{2,n} \left(l_n - \frac{t_n^{\text{MAP}} f_n^{\text{max}}}{c_n} \right) - \gamma_{3,n} t_n^{\text{MAP}} + \gamma_{4,n} (t_n^{\text{MAP}} - \tau) \end{aligned}$$

with $\gamma_{1,n}, \gamma_{2,n}, \gamma_{3,n}, \gamma_{4,n} \geq 0$ the Lagrange multipliers. The KKT conditions are then given by

$$\frac{\partial \mathcal{L}_{1,n}}{\partial l_n} = 3 \frac{\kappa_n c_n^3 l_n^2}{(t_n^{\text{MAP}})^2} + \alpha \mu_n - \lambda - \gamma_{1,n} + \gamma_{2,n} = 0 \quad (28)$$

$$\frac{\partial \mathcal{L}_{1,n}}{\partial t_n^{\text{MAP}}} = -2 \frac{\kappa_n c_n^3 l_n^3}{(t_n^{\text{MAP}})^3} + \beta_n - \gamma_{2,n} \frac{f_n^{\text{max}}}{c_n} - \gamma_{3,n} + \gamma_{4,n} = 0 \quad (29)$$

with the complementary slackness conditions

$$\gamma_{1,n} l_n = 0, \quad (30)$$

$$\gamma_{2,n} \left(l_n - \frac{t_n^{\text{MAP}} f_n^{\text{max}}}{c_n} \right) = 0, \quad (31)$$

$$\gamma_{3,n} t_n^{\text{MAP}} = 0, \quad (32)$$

$$\gamma_{4,n} (t_n^{\text{MAP}} - \tau) = 0. \quad (33)$$

We first obtain (19), (20) and (22) using condition (28) and complementary slackness conditions (30) and (31). Substituting (19) in (29) and defining $\rho_{1,n} = \gamma_{4,n} - \gamma_{3,n}$, we then obtain (21) using complementary slackness conditions (32) and (33).

B. Proof of Lemma 4

Problem (17) being convex, the optimal solution satisfies the KKT conditions. The Lagrangian of problem (17) is given by

$$\begin{aligned} \mathcal{L}_{2,n} = & E_n + t_n^{\text{SHU}} P_n^c - \mu_n t_n^{\text{SHU}} r_n \left(\frac{E_n}{t_n^{\text{SHU}}} \right) + \beta_n t_n^{\text{SHU}} - \delta_{1,n} E_n \\ & + \delta_{2,n} (E_n - t_n^{\text{SHU}} p_n^{\max}) - \delta_{3,n} t_n^{\text{SHU}} + \delta_{4,n} (t_n^{\text{SHU}} - \tau) \end{aligned}$$

with $\delta_{1,n}, \delta_{2,n}, \delta_{3,n}, \delta_{4,n} \geq 0$ the Lagrange multipliers. The KKT conditions are then given by

$$\frac{\partial \mathcal{L}_{2,n}}{\partial E_n} = 1 - \delta_{1,n} + \delta_{2,n} - \mu_n \frac{\frac{h_n}{N_0}}{1 + \frac{E_n}{t_n^{\text{SHU}}} \frac{h_n}{BN_0}} = 0 \quad (34)$$

$$\begin{aligned} \frac{\partial \mathcal{L}_{2,n}}{\partial t_n^{\text{SHU}}} = & \mu_n \frac{\frac{E_n}{t_n^{\text{SHU}}} \frac{h_n}{N_0}}{1 + \frac{E_n}{t_n^{\text{SHU}}} \frac{h_n}{BN_0}} - \mu_n r_n \left(\frac{E_n}{t_n^{\text{SHU}}} \right) + P_n^c + \beta_n \\ & - \delta_{2,n} p_n^{\max} - \delta_{3,n} + \delta_{4,n} = 0 \end{aligned} \quad (35)$$

with the complementary slack conditions

$$\delta_{1,n} E_n = 0 \quad (36)$$

$$\delta_{2,n} (E_n - t_n^{\text{SHU}} p_n^{\max}) = 0 \quad (37)$$

$$\delta_{3,n} t_n^{\text{SHU}} = 0 \quad (38)$$

$$\delta_{4,n} (t_n^{\text{SHU}} - \tau) = 0. \quad (39)$$

We first obtain (23), (24) and (26) using condition (34) and complementary slackness conditions (36) and (37). Substituting (23) in (35) and defining $\rho_{2,n} = \delta_{4,n} - \delta_{3,n}$, we then obtain (25) using complementary slackness conditions (38) and (39).

C. Proof of Lemma 5

Problem (18) being convex, the optimal solution satisfies the KKT conditions. The Lagrangian of problem (18) is given by

$$\begin{aligned} \mathcal{L}_3 = & \sum_{n=1}^N \frac{\kappa_n c_n^3 T^3}{(t^{\text{RED}})^2} + \beta_n t^{\text{RED}} + \epsilon_1 \left(\max_n \left\{ \frac{c_n T}{f_n^{\max}} \right\} - t^{\text{RED}} \right) \\ & + \epsilon_2 (t^{\text{RED}} - \tau) \end{aligned}$$

with $\epsilon_1, \epsilon_2 \geq 0$ the Lagrange multipliers. The KKT conditions are then given by

$$\frac{\partial \mathcal{L}_3}{\partial t^{\text{RED}}} = \epsilon_2 - \epsilon_1 - 2 \left(\frac{T}{t^{\text{RED}}} \right)^3 \sum_{n=1}^N \kappa_n c_n^3 + \sum_{n=1}^N \beta_n = 0 \quad (40)$$

with the complementary slackness conditions

$$\epsilon_1 \left(\max_n \left\{ \frac{c_n T}{f_n^{\max}} \right\} - t^{\text{RED}} \right) = 0 \quad (41)$$

$$\epsilon_2 (t^{\text{RED}} - \tau) = 0. \quad (42)$$

Condition (40) together with complementary slackness conditions (41) and (42) allow us to obtain (27).

REFERENCES

- [1] M. Chiang and T. Zhang, “Fog and iot: An overview of research opportunities,” *IEEE Internet of Things Journal*, vol. 3, no. 6, pp. 854–864, Dec 2016.
- [2] A. Mammela and A. Anttonen, “Why will computing power need particular attention in future wireless devices?” *IEEE Circuits and Systems Magazine*, vol. 17, no. 1, pp. 12–26, Firstquarter 2017.
- [3] S. Barbarossa, S. Sardellitti, and P. Di Lorenzo, “Communicating while computing: Distributed mobile cloud computing over 5g heterogeneous networks,” *IEEE Signal Processing Magazine*, vol. 31, no. 6, pp. 45–55, Nov 2014.
- [4] H. T. Dinh, C. Lee, D. Niyato, and P. Wang, “A survey of mobile cloud computing: architecture, applications, and approaches,” *Wireless Communications and Mobile Computing*, vol. 13, no. 18, pp. 1587–1611, 2013. [Online]. Available: <https://onlinelibrary.wiley.com/doi/abs/10.1002/wcm.1203>
- [5] Y. C. Hu, M. Patel, D. Sabella, N. Sprecher, and V. Young, “Mobile edge computing a key technology towards 5g,” *ETSI white paper*, 2015.
- [6] Y. Mao, C. You, J. Zhang, K. Huang, and K. B. Letaief, “A survey on mobile edge computing: The communication perspective,” *IEEE Communications Surveys Tutorials*, vol. 19, no. 4, pp. 2322–2358, Fourthquarter 2017.
- [7] P. Mach and Z. Becvar, “Mobile edge computing: A survey on architecture and computation offloading,” *IEEE Communications Surveys Tutorials*, vol. 19, no. 3, pp. 1628–1656, thirdquarter 2017.
- [8] E. El Haber, T. M. Nguyen, and C. Assi, “Joint optimization of computational cost and devices energy for task offloading in multi-tier edge-clouds,” *IEEE Transactions on Communications*, vol. 67, no. 5, pp. 3407–3421, May 2019.
- [9] D. Liu, B. Chen, C. Yang, and A. F. Molisch, “Caching at the wireless edge: design aspects, challenges, and future directions,” *IEEE Communications Magazine*, vol. 54, no. 9, pp. 22–28, Sep. 2016.
- [10] J. Dean and S. Ghemawat, “Mapreduce: Simplified data processing on large clusters,” in *OSDI’04: Sixth Symposium on Operating System Design and Implementation*, San Francisco, CA, 2004, pp. 137–150.
- [11] A. Paris, H. Mirghasemi, I. Stupia, and L. Vandendorpe, “Energy-efficient edge-facilitated wireless collaborative computing using map-reduce,” in *2019 IEEE 20th International Workshop on Signal Processing Advances in Wireless Communications (SPAWC)*, July 2019, pp. 1–5.
- [12] S. Li, Q. Yu, M. A. Maddah-Ali, and A. S. Avestimehr, “A scalable framework for wireless distributed computing,” *IEEE/ACM Transactions on Networking*, vol. 25, no. 5, pp. 2643–2654, Oct 2017.
- [13] M. Kiamari, C. Wang, and A. S. Avestimehr, “Coding for edge-facilitated wireless distributed computing with heterogeneous users,” in *2017 51st Asilomar Conference on Signals, Systems, and Computers*, Oct 2017, pp. 536–540.
- [14] S. Li, M. A. Maddah-Ali, Q. Yu, and A. S. Avestimehr, “A fundamental tradeoff between computation and communication in distributed computing,” *IEEE Transactions on Information Theory*, vol. 64, no. 1, pp. 109–128, Jan 2018.

- [15] F. Li, J. Chen, and Z. Wang, "Wireless MapReduce Distributed Computing," 2018. [Online]. Available: <http://arxiv.org/abs/1802.00894>
- [16] X. Cao, F. Wang, J. Xu, R. Zhang, and S. Cui, "Joint computation and communication cooperation for energy-efficient mobile edge computing," *IEEE Internet of Things Journal*, vol. 6, no. 3, pp. 4188–4200, June 2019.
- [17] C. You and K. Huang, "Exploiting non-causal cpu-state information for energy-efficient mobile cooperative computing," *IEEE Transactions on Wireless Communications*, vol. 17, no. 6, pp. 4104–4117, June 2018.
- [18] Z. Sheng, C. Mahapatra, V. C. M. Leung, M. Chen, and P. K. Sahu, "Energy efficient cooperative computing in mobile wireless sensor networks," *IEEE Transactions on Cloud Computing*, vol. 6, no. 1, pp. 114–126, Jan 2018.
- [19] D. Wu, F. Wang, X. Cao, and J. Xu, "Wireless powered user cooperative computation in mobile edge computing systems," 2018.
- [20] A. Mtibaa, A. Fahim, K. A. Harras, and M. H. Ammar, "Towards resource sharing in mobile device clouds: Power balancing across mobile devices," *SIGCOMM Comput. Commun. Rev.*, vol. 43, no. 4, p. 5156, Aug. 2013. [Online]. Available: <https://doi.org/10.1145/2534169.2491276>
- [21] L. Pu, X. Chen, J. Xu, and X. Fu, "D2d fogging: An energy-efficient and incentive-aware task offloading framework via network-assisted d2d collaboration," *IEEE Journal on Selected Areas in Communications*, vol. 34, no. 12, pp. 3887–3901, Dec 2016.
- [22] M. S. Andersen, J. Dahl, and L. Vandenberghe, "CVXOPT: A Python package for convex optimization." [Online]. Available: <https://cvxopt.org/>